Submerged shoreline preservation and ravinement during rapid postglacial sea-level rise and subsequent "slowstand"

Lauren Pretorius, Andrew Green and Andrew Cooper

ABSTRACT

Submerged shorelines hold much potential for examining the interplay between the rate of sea-level rise and geomorphic setting, and informing the development of models of contemporary shoreline behavior. This paper describes the sedimentary architecture of a submerged barrier shoreline complex off Durban, South Africa. The complex consists of several barriers that have survived the postglacial transgression and associated erosive ravinement processes. The main shoreline sequence (–60 m) dates to 11,690 ± 90 calibrated (cal) yr B.P. and rests on a Pleistocene lagoonal deposit (35,395 ± 592 cal yr B.P.). The entire barrier shoreline complex is truncated by a strongly diachronous wave ravinement surface. The ravinement surface seaward of the main –60 m shoreline is steep, but the gradient declines across and landward of the subordinate landward shoreline complexes. The steep ravinement surface is attributed to fast sea-level rise (possibly associated with meltwater pulse 1B), while the gentle ravinement surface is associated with a subsequent slowing of the rate of sea-level rise (to 0.15 mm yr–1). Preservation of the main barrier and backbarrier deposits through overstepping is associated namely with rapid transgression and increased back-barrier accommodation. The smaller barriers landward of the main barrier were preserved through overstepping related to gentle antecedent gradients, despite more intense

ravinement during a very slow rise in sea level (slowstand). This process was assisted by a sediment deficit. The resulting post-transgressive drape is also influenced by antecedent topography created by the barriers themselves; damming along the landward sides of overstepped barriers thickens the drape and creates a temporal disconnect between the migration of the shoreface and more landward elements of the littoral system. In examining the rates of shoreline migration associated with the overstepped barrier system, these are far greater than those calculated for the predicted rates of shoreline change on similarly steep coastal profiles. Future rates of shoreline migration appear to be insufficient to cause overstepping, and rollover or erosional responses are more likely.

INTRODUCTION

Understanding the response of barrier shorelines to contemporary and future sea-level rise is of major societal importance and has been the subject of several recent modeling studies (e.g., Lorenzo-Trueba and Ashton, 2014; Brenner et al., 2015) that seek to replace the antiquated and obsolete Bruun rule (Cooper and Pilkey, 2004). There is, however, a limited range of contemporary and historical sea-level and geomorphic contexts of modern shorelines against which to test these models. Most studies to date are on low-gradient, coastal plain settings, particularly of the eastern United States (e.g., Engelhart et al., 2009; Thieler and Ashton, 2011), which are not representative of all contemporary shorelines. Stratigraphic evidence from submerged shorelines on the continental shelf holds the potential to elucidate the response of the entire littoral zone (shoreface through barrier to back-barrier) as it migrates up profile under a range of sea-level and geomorphic scenarios. The detailed sedimentary and stratigraphic architecture of submerged shoreline deposits thus provides information on the rate of sea-level rise (e.g., overstepping vs. rollover; e.g., Mellett et al.,

2012), the rate and effectiveness of transgressive ravinement processes (e.g., Davis and Clifton, 1987), and the ways in which these processes interact to produce and preserve facets of submerged shorelines on continental shelves worldwide (e.g., Green et al., 2014). By examining relict shoreline features, more parallels between modeling attempts and real-world scenarios can be drawn, and the long-term controls on shoreline migration and preservation can be better understood.

This paper presents a detailed stratigraphic architecture and associated chronology of a submerged shoreline complex first documented by Green et al. (2013a). The aim here is to describe the stratigraphic facets produced in a submerged shoreline as a response to varying rates of relative sea-level rise, antecedent morphology, and intensity of ravinement. For the first time, we describe associated core data from the back-barrier environments of this shoreline complex and discuss the timing and significance of ravinement processes relative to its preservation. The data include the period around meltwater pulse 1B and cast light on littoral zone behavior during major variations in the rate of sea-level rise. The area itself is of particular significance in that geophysical model predictions suggest a Holocene sea-level history close to that of the eustatic sea-level curve (Milne and Mitrovica, 2008).

REGIONAL SETTING

The KwaZulu-Natal continental shelf (Fig. 1), offshore Durban, is narrow (~20 km) compared to the world average of 78 km (Shepard, 1963; Kennett, 1982). The shelf break occurs at a depth of ~100 m and marks a gradual transition from the shelf to the upper slope (Green et al., 2013b). The resulting shelf gradient is steep (~0.6°) compared to the worldwide average (0.116°; Shepard, 1963). The coastline in the study area is intersected by two

estuarine systems: the Mgeni River in the north (Cooper, 1993), and the Durban harbor complex in the south (Green and Garlick, 2011). Despite the two fluvial inputs, sediment supply to the shelf has been particularly low since the Pliocene, and the margin is considered sediment starved (Green and Garlick, 2011). The KwaZulu-Natal coast is upper microtidal, with a spring tidal range of 1.8 m, and exposed to a high degree of wave activity throughout the year (significant wave height, Hs = 1.8 m; Moes and Rossouw, 2008). The outer shelf is swept by the energetic Agulhas Current, a poleward-flowing western boundary current that is considered responsible for the general sediment-starved nature of the area (Martin and Flemming, 1988; Green and MacKay, 2016).

The study area is underlain by Cretaceousage siltstones (Green and Garlick, 2011; Cawthra et al., 2012; Green et al., 2013a) into which several valleys have incised (Green et al., 2013b). These valleys were filled by sediment during the late Pleistocene–Holocene when sea levels rose after the Last Glacial Maximum (LGM) at 18,000 yr B.P., when they were ~120 m lower than present (Ramsay andCooper, 2002). Superimposed on the Cretaceous basement, there are several submerged, shore-parallel ridge structures composed of eolianite and beachrock material (Green et al., 2013a). These ridges preserve former shoreline positions, overlie the valley networks, and are considered to be late Pleistocene to Holocene in age (Martin and Flemming, 1987). A Holocene sediment wedge blankets the shelf in the form of a semicontinuous inner- to midshelf sediment wedge, with outcrops of the Cretaceous basement exposed on the outer shelf due to the winnowing action of the Agulhas Current (Flemming and Hay, 1988; Birch, 1996). Very few published data exist from the east coast of South Africa concerning lower-than present sea levels spanning the last interglacial period to present day. Isolated wetland peats found in incised valley fills from the Durban area yielded ages of 45,200 ± 2000 yr B.P. (uncal) and 39,100 ± 1530 yr B.P. (uncal) from elevations of –

52 and –46 m mean sea level (MSL), respectively (Ramsay and Cooper, 2002). An undated storm beach deposit was identified by Green and Uken (2005) in a submarine cave at an elevation of –125 m MSL and attributed to the LGM shoreline. With regard to the deglacial sea-level history, Ramsay and Cooper (2002) documented a number of Holocene-aged sealevel indicators from varying depths, many of which have large assumed vertical errors. Nevertheless, the general picture that emerges is of a rapid deglacial sea-level rise that ended ~6000 yr ago when sea levels stabilized around present day MSL (Fig. 2; Ramsay and Cooper, 2002).

METHODS

The subsurface geomorphology and sedimentary architecture of the study area were examined using two methods. High-resolution seismic profiles were collected using a 200J boomer system, coupled to an 18 element hydrophone array. The data were collected using HypackTM and processed with in-house designed software that included the application of time-varied gains, band-pass filtering (300–1200 Hz), swell filtering, and manual seabed tracking. Streamer layback and antenna offset corrections were applied to the digitized data set, and constant sound velocities in water (1500 m/s) and sediment (1600 m/s) were used to extrapolate all time-depth conversions. The vertical resolution
of these data is ~50 cm.

Ultrahigh-resolution seismic profiles were collected using a PARASOUND parametric echosounder aboard the research vessel (RV) Meteor, during cruise M102. The low-frequency output (0.5 kHz) was selected due to signal attenuation of the higher-frequency spectra. The data were processed with high and low band-pass filtering

and gain applications, then exported as SEGY data for visualization in Kingdom Suite. These data resolve to ~10 cm in the vertical domain. The subsurface interpretations were further bolstered by the incorporation of multibeam bathymetry data described by Green et al. (2013a).

Three cores were acquired in order to examine the subsurface stratigraphy of the study area and to conduct ground-truthing of the seismic results. Cores were collected using a 100-mm-diameter, 5-m-long marine vibrocorer from water depths of between 30 and 60 m, marking the proximal and distal portions along the incised valley profile (Fig. 1) described by Green et al. (2013a). The cores were split, photographed, and logged according to standard sedimentological procedures, and the cores were subsampled for accelerator mass spectrometry (AMS) C14 dating. The material sampled for AMS dating is described in Table 1. Whole shells (particularly articulated bivalves) that were used for dating purposes were sampled from life position and specifically selected where color bleaching was limited. All AMS dates were calibrated using OXCAL software (Ramsey, 2001) and the marine13.14c calibration model (Reimer et al. 2013).

RESULTS

Seismic Stratigraphy

The oldest unit, or acoustic basement, of the study area is composed of Cretaceous-age siltstones (e.g., Green and Garlick, 2011), upon which a thinly developed cover succession rests. The shallow stratigraphy consists of four units, separated by various unconformity surfaces (Table 2). An uneven, high-amplitude reflector (surface 1) truncates the Cretaceous-

age strata, occurring across the midshelf (Figs. 3–6). This surface forms multiple incisions into the underlying basement in the form of several incised valleys (Figs. 4B and 6B; Fig. 6A, inset 1), which may reach 200 m in width and have valley reliefs of up to 30 m. These valleys are filled by a series of low-amplitude, draped reflector packages (unit 1). These onlap surface 1 (Figs. 4B and 6B; Fig. 6A, inset 1) and are truncated or toplapped by a very rugged, high-amplitude surface (surfaces 2 and 3; Figs. 4A and 4B). Surface 2 occurs as a rugged, very high-amplitude reflector that is only preserved as a capping horizon associated with the incised valley fills of unit 1 in the proximal inner shelf (Fig. 4A).

Surface 3 is an uneven, high-amplitude reflector that erosionally truncates the upper portions of unit 1 and can merge with surface 1 on the valley interfluves to form a composite surface (Fig. 4B). Proximally, it is separated from the underlying surface 2 by a very thin (~1 m) layer of material. Surface 3 forms the distally capping unconformity surface of the incised valley fills of unit 1. Seaward of the 60 m isobath, it dips steeply seawards (0.89°) and flattens to landward, with a significantly more gentle profile (0.18°; Figs. 3–5).

Unit 2 consists of a series of high-relief pinnacles and ridges with a high-amplitude, chaotic internal reflector configuration that often appears acoustically opaque. Acoustic masking of the underlying stratigraphy is prominent (Figs. 3A–3C, 4C, 5A, 5C, and 6B, insets 1–3). The bases of this unit occur at consistent depths of ~60 m and ~40 m, with the most prominent ridges occurring at ~60 m basal depth (Figs. 3, 4, and 6B). Lower-resolution seismic tools reveal unit 2 to rest on surface 1 (Figs. 6A–6C). On the valley interfluves, surface 3 has truncated the pinnacles of unit 2.

Unit 3 occurs as acoustically opaque material with little or no internal structure. This unit rests on surface 1 and onlaps unit 2. This unit shows a landward-prograding, moderate-amplitude shingled reflector configuration (Figs. 4E and 5B). Unit 3 is associated with the landward side of the pinnacles of unit 2 and may reach the seaward side of adjacent unit 2 structures up profile in the more distal areas (Fig. 4C). This unit is mainly restricted to the midshelf region and is truncated by surface 3.

Unit 4 forms a seaward-pinching wedge that locally onlaps and downlaps both units 2 and 3 (Figs. 3 and 6C). The internal reflector configuration may become increasingly sigmoidal, downlapping surface 3 where the wedge thickens to landwards. The wedge of unit 4 preferentially accumulates as thicker deposits on the seaward flanks of the ridges of unit 2, where it aggradationally onlaps the pinnacle and ridge features (Figs. 6A, inset 3, and 6B, inset 1). Unit 4 may also occur as a series of highamplitude draped reflectors that onlap adjoining ridges, forming intrasaddle depression fills. On this basis, three different subunits may be further identified with respect to their seismic characteristics and morphology. These manifest as different seismic reflector configurations that grade into one another downdip, yet may have no definable separating unconformity surfaces.

Subunit 4.1 is a package of continuous, moderate- amplitude, seaward-prograding sigmoid reflectors that downlap surface 3 (Figs. 3A, 4B, and 5C). In the most seaward/distal portions of the seismic coverage, the sigmoid prograding to oblique tangential reflectors become more steeply seaward dipping (Figs. 3A–3C, 4B, 6A, inset 3, 6B, inset 1, and 6C, insets 1, 3, and 5).

Occasional subhorizontal to subparallel reflectors are apparent; these onlap the pinnacles of unit 2 and downlap the underlying surface (Figs. 4C, 4E, 4F, and 5B). In some cases, this subunit shows an acoustically opaque character and can be identified by the overall geometry of the package and its downlap relationship with unit 3 (Fig. 4E). This subunit is occasionally truncated at the top by modern-day erosional processes associated with the seafloor.

Resting above surface 3 and restricted to the inner-shelf region is subunit 4.2. This subunit grades from the seaward-prograding reflectors of subunit 4.1 into discontinuous, moderate amplitude, contorted to segmented subparallel reflectors (Fig. 4B). The subparallel reflectors are most prominent where the underlying topography of surface 3 dips landward. Subunit 4.2 subsequently grades into subunit 4.1 when the orientation of the dip of surface 3 changes to a seaward direction (Fig. 4).

Subunit 4.3 lies on the seaward side of the pinnacle structures of unit 2 and rests on surface 3. This subunit displays a range of reflector configurations with a continuous, moderate amplitude, landward-prograding oblique parallel to divergent reflector configuration being the most common (Figs. 4D, 5A, and 5C). Subunit 4.3 tends to abut the landward side of unit 2 pinnacles in the inner-shelf section with reflectors downlapping surface 3 (Fig. 4D).

Lithostratigraphy

Core GeoB18303

Core GeoB18303 was acquired in the landward lee of the most-seaward outcrop of unit 2.

This core intersects seismic units 1 and 4 in the more distal part of the incised valley system formed in surface 1. Facies A1 of core GeoB18303 is composed of fine sand with minor silt and occasional lenses of medium sand– and coarse sand–sized shell debris (Fig. 7A). This facies is separated from the overlying facies by a sharp contact. Facies B1 consists of very coarse, poorly sorted, gravel-rich sand that coarsens upward. The overlying facies C1 similarly consists of very coarse, poorly sorted, gravel-rich sand but displays a fining-upward pattern.

In facies C1, shell hashes consisting of barnacle-encrusted oysters of large cobble size are encountered. The base of facies C1 is marked by a cobble-size clast of semiconsolidated material of similar composition to the surrounding sediment (Fig. 7A). The upper portion of this unit hosts a 10-cm-diameter muddy ripup clast (–1.90 m; Fig. 7A). This unit is truncated by an erosional contact, overlain by facies D1, consisting of medium sand with abundant shell debris. Facies E1 consists of gravel-bearing, poorly sorted, coarse sand with abundant shell debris and a sharp upper contact. This is overlain by two fining-upward cycles (facies F1 and G1) of gravel-bearing, poorly sorted, coarse sand with abundant shell hash and sharp upper contacts.

Core GeoB18304

Core GeoB18304 (Fig. 7B) is the most proximal of the cores taken, extracted from a water depth of 40 m, and representing the lithostratigraphic equivalent of seismic units 1 and 4.

Facies A2 is composed of medium sand with silt and isolated shell debris. This facies coarsens upward into coarse sand and is truncated by an erosional contact. The overlying

units represent alternating packages of coarser material, usually consisting of shell hash (facies B2), interbedded with shell fragment–rich medium sands. These are occasionally planar laminated (facies C2).

Facies D2 represents a coarser-grained variant of C2, with pebble-sized shell debris forming layers up to 7 cm thick. The most prominent horizon of facies D2 occurs ~310 cm down core and is overlain by several thin alternations of facies B2 and C2. This is capped by an upward coarsening unit (~270 cm thick) of facies C2, A2, and B2.

Core GeoB18302

Core GeoB18302 was retrieved from a saddle between two outcrops of unit 2 (Fig. 7C). The core penetrated 6 m of the stratigraphy and intersected unit 4 (subunit 4.3). The lowermost unit encountered was a stiff, organic-rich mud (facies A3) unresolved in the seismic data. This was truncated by a strongly erosional surface and overlain by facies B3. The majority of the core consisted of angular and poorly consolidated fragments of weathered calcareous sandstone in a muddy matrix (facies B3). The sandstone fragments consisted of calcite-cemented medium sand with a high abundance of shell debris. Fragments of bivalves, serpulid worms, and oyster shells are common.

Chronostratigraphic Framework and Correlation to Seismic Stratigraphy

AMS radiocarbon dates from several key stratigraphic horizons are shown in Table 1.
The oldest material cored is stiff clay dated to 35,395 ± 592 cal yr B.P. This occurs as a very

thin drape of material, unresolvable by the ultrahigh- resolution seismics due to the overlying rubble horizon of reworked material from unit 2. The upper packages of unit 1 (very coarse sand of facies B1 and B2) had ages that spanned from 13,300 ± 70 cal yr B.P. to 6480 ± 40 cal yr B.P., younging proximally up profile. Surface 3 is dated in the proximal areas at 5530 ± 40 cal yr B.P. Distally, the immediate underlying horizon beneath surface 3 is dated at 11,690 ± 90 cal yr B.P. The overlying units are correlated with the coarse sandy facies of subunit 4.1 and date from 3835 ± 35 to 2845 ± 30 cal yr B.P.

DISCUSSION

Seismic Stratigraphic Interpretation

Unit 1 consists of late Pleistocene– to Holocene- aged incised valley fill sediments, as identified by Green et al. (2013a, 2013b). These sediments were deposited during the transgression that followed the LGM. These overlie surface 1, onlap the valley walls, and are capped by surface 2, a low-relief erosional surface that truncates the valley fill in the proximal portions of the valley (Figs. 4, 6A, and 6B). GeoB18304 and GeoB18303 both penetrate the upper valley fill package. GeoB18303 intersects the outer segment of the incised valley profile and marks a transition from fine sandy material to very coarse sand. Despite not being clearly imaged in the ultrahigh-resolution seismic data, it appears that the two facies (A1 and B1) comprise the central estuarine basin fill and overlying sandy flood-tide deltaic complex, respectively. Similar lithofacies arrangements are described by Dabrio et al. (2000) and Nichol et al. (1997) from other incised valley fills. These are separated by the tidal ravinement surfaces observed in the more proximal areas, which are not as well preserved along the distal portions of the valley system. Surface 2 is consequently

interpreted in a similar manner as the tidal ravinement surface within the proximal middle segment of the incised valley.

Unit 2 is welded onto the interfluves of surface 1. Its ridge-like morphology and architecture, in addition to the acoustic opacity of the unit, is similar to calcareous cemented sandstone features found on shelves worldwide (e.g., Carter et al., 1986; Locker et al., 1996; Jarrett et al., 2005; Storms et al., 2008; Brooke et al., 2014). These are equivalent to coastal dunes and their nearshore equivalents (barrier complexes) that have been calcified and later inundated (e.g., Ramsay, 1994; Locker et al., 1996). Petrographic observations of samples collected during scuba campaigns from the shallower portions of unit 2 revealed a meteoric cementation of eolian sands (Richardson, 2005) and thus confirmed the coastal dune/barrier interpretation.

The intensely erosive, high-relief upper bounding surface of unit 2 (surface 3) is interpreted as the wave ravinement surface formed during shoreface translation over the barrier shoreline profile of unit 2 (e.g., Cattaneo and Steel, 2003). The wave ravinement surface displays a seaward-dipping geometry and occurs as a shelly hash, with pebbles and occasional eolianite cobbles derived from unit 2 (Figs. 7A–7C). The deposits comprising this surface are similar to the erosive lag surfaces ascribed to the processes of wave ravinement as recognized by other authors (e.g., Goff et al., 2010; Zecchin and Catuneanu, 2013). In examining the ages of sediment directly above or beneath this surface from the distal to proximal areas, it is clear that the surface is strongly diachronous; wave ravinement had already begun at 11,690 ± 90 cal yr B.P. at the 60 m water depth site and continued in the proximal shelf until at least 5530 ± 40 cal yr B.P.

Unit 3 takes the form of small-scale onlapping, low-amplitude reflector drapes that rest within the depressions of saddles between successive outcrops of unit 2. The seismic characteristics of unit 3 suggest a low-energy environment of deposition. Unit 3 drapes the subaerial unconformity (surface 1) and is truncated by the wave ravinement surface (surface 3). Based on the geometry of the deposit (onlapping drape behind the barriers of unit 2), its position beneath the wave ravinement surface, and its location relative to the barrier (unit 2), this unit is interpreted as a back-barrier lagoonal deposit transgressed during wave base translation up the profile. Unit 4 comprises an unconsolidated sandy wedge of Holocene-aged sand and shell debris, with occasional muddy rip-up clasts (likederived from unit 3) and eolianite rubble of unit 2. The timing of the wedge spans the early Holocene, where the basal ravinement surface is dated at ca. 11 600 cal yr B.P. to present day.

Previously, the small progradational packages within this wedge were interpreted as regressive packages formed during slower rates of the Holocene transgression, stillstand, or smallscale regressions (Green and Garlick, 2011). Using new core data, higher-resolution seismic data, and geochronological constraints, a more detailed interpretation of the postravinement blanket can be made. Subunit 4.1 forms part of the modern lower shoreface. It rests on relatively flat portions of the wave ravinement surface and onlaps the seaward margins of the barrier complex of unit 2.

Unit 2 disrupts the connection of these deposits from the upper shoreface profile. Unlike the transgressive healing phase deposits recognized by Cattaneo and Steel (2003) and Zecchin and Catuneanu (2013), subunit 4.1 comprises a disaggregated series of isolated deposits that occur sporadically along the seaward-sloping wave ravinement surface.

Subunit 4.2 displays discontinuous, wavy, and chaotic seismic reflector characteristics. Similar reflector configurations were described by Green et al. (2012) for the shoreface of Durban, where they interpreted these seismic reflectors, together with core data, to represent stormgenerated reworking of the lower shoreface. The position of these deposits at ~30 m water depth or shallower supports this hypothesis.

Subunit 4.3 occurs as a thick (~3 m) package of material, often within saddles of the barriers of unit 2. In isolated depressions, this unit comprises packages of rubble derived from unit 2, located only in the most proximal back-barrier environments (Figs. 5 and 7C). Subunit 4.3 progrades landward, suggestive of phases of accumulation of material in the lee of the cemented barrier via storm overwashing processes during the landward migration of the shoreface over the pinnacles of the unit 2 barriers.

Shoreline Genesis

The stratigraphic and chronological evidence indicates the presence of two temporally distinct but superimposed shorelines at approximately –60 m. The first includes the stiff clay dated at 35,395 cal yr B.P. This is correlated regionally with identical deposits, interpreted as lagoonal, at similar depths ~75 km north of the study area (Felhaber, 1984; Flemming and Hay, 1988; Fig. 2). The northern deposits are palimpsest features. Green and MacKay (2016) related the exposure of these deposits to ravinement processes during deglacial sea-level rise, a process similarly mirrored by the Durban example revealed here. In this case, the lagoonal deposits are truncated by the wave ravinement surface (surface 3) and are overlain by rubble facies derived from unit 2.

Based on the dating of the organic material in the lagoonal muds offshore of Durban, this shoreline was exposed during oxygen isotope stage 3 as sea levels dropped to the LGM (Ramsay and Cooper, 2002) and survived subaerial exposure for ~20,000 yr until it was reflooded during the postglacial marine transgression (Fig. 2). It appears that the lagoonal facies are the sole remnant of this shoreline, where the associated barrier deposits (eolianites) did not survive the 20,000 yr of subaerial exposure.

We consider the second shoreline at 60 m water depth to be the result of a barrier-building event that occurred during the occupation of sea level at ~60 m during sea-level rise of the last deglaciation. Units 2 and 3, the preserved barrier and back-barrier sequences, respectively, occur above the LGM-aged channels in the area (Green et al., 2014) and support a postglacial age for this subsequent shoreline. As the barrier built, the back-barrier areas became more isolated from marine influences, and the incised valley fill became progressively finer (facies A1; Fig. 7A), a process Green et al. (2013a) associated with lagoonal segmentation and which Cooper et al. (2011) reported in contemporary local lagoons. The overlying seaward, upper packages of the incised valley fills of the underlying unit 1 were deposited at 11,690 ± 90 cal yr B.P. and were likely coeval with the last stages of the seaward barrier development when flood tide deltas would be best developed. The barrier had at this point grown significantly, modifying the tidal prism by constricting the inlet and producing a series of localized flood tide deltaic packages in the upper valley fill. These deposits mark the final point in the system evolution before the barrier was eroded and ravinement began during rising sea level.

The shoreline was then transgressed as the wave base translated landward, and its remnants

were ultimately covered by material mid- to late Holocene in age (the contemporary shoreface; Fig. 7; Table 1). Green et al. (2013a) and Salzmann et al. (2013) postulated that a regional series of barriers formed during a very slow rise in global sea level (slowstand, cf. Kelley et al., 2010) at between 12.7 and 11.6 k.y. B.P., and the dates presented here provide the first confirmation of this hypothesis.

The subsidiary shorelines that occur landward of the main barrier shoreline appear to be back-stepped remnants of smaller barriers that formed during transgression up to a depth of 28 m. These are likely to have formed after the initial slowstand that allowed the main barrier to form, and they mark a second, slow migration of the shoreline over the coastal profile at shallower depths, producing smaller, more poorly preserved barrier remnants.

Preservation by Overstepping

Preservation of the –60 m eolianite barrier shoreline deposits on this high-energy shelf appears to have been contingent upon shelf gradient; erosion by landward migration of a shoreline across a high-gradient continental shelf is typically more powerful than across a low-gradient shelf (Cattaneo and Steel, 2003). This is because although the rate of sea-level rise may be constant, the steeper gradient allows the wave base to occupy the same space for longer time periods during wave ravinement (Davis and Clifton, 1987). Despite the steep shelf gradient and consistently high wave energy of the study area, barrier shoreline and back-barrier deposits have been remarkably well preserved. The rate of relative sea-level rise, the grain size of the deposits, the tidal range, and barrier volume will determine the extent of preservation and the nature of the preserved deposits during sealevel rise over the coastal profile (Storms et al., 2008). Of these criteria, we consider the rate of sea-level rise as the

most important control in this area (e.g., Green et al., 2013a). This is particularly so in the context of the small tidal range, the sandy nature of the barrier material, and the small volume of sand in the barrier (cf. Green et al., 2013a). The more rapid the rate of sea-level rise, the greater is the likelihood that the shoreline, barrier, and back-barrier deposits will be overstepped (Belknap and Kraft, 1981; Forbes et al., 1995; Storms et al., 2008).

We show clear evidence for the existence of intervals of rapid sea-level rise in the remarkable preservation of back-barrier deposits. If the rate of sea-level rise was slow, the back-barrier lagoonal deposits would have been eroded and reworked to a large extent by bay ravinement processes, leaving behind only sparse remnants (if any) of the postglacial back-barrier lagoon system. These deposits are best preserved if there is no migration of the barrier landward (i.e., overstepping) and if there is rapid creation of accommodation in the back-barrier (Forbes et al., 1995; Mellett et al., 2012). This has the combined effect of dampening the effects of both tidal and wave ravinement.

The effect of increasing back-barrier accommodation can be amplified by a reduced shoreline gradient (e.g., Fig. 4). Such a scenario is considered to foster overstepping and preservation of the back-barrier profile (Storms et al., 2008). Lorenzo-Trueba and Ashton (2014) demonstrated that this factor alone may account for the overstepping process without any associated rapid rise in sea level. However, when placed into the context of the core data and geochronology, we prefer the former argument of an increased rate of sea-level rise, acting in combination with the influence of the subdued antecedent backbarrier topography, as being responsible for overstepping in this case. The age of sediment immediately underlying the wave ravinement surface in the most seaward back-barrier areas is 11,690 ± 90 cal yr B.P., fronted by the main shoreline/barrier complex at a depth of 60 m. This closely matches the

suspected rapid rise in global sea levels from water depths of 60 m to 48 m between 11,500 and 11,200 cal yr B.P. (Liu and Milliman, 2004). We consider that
the ravinement surface in the back-barrier was formed during this rapid rise of sea level over the barrier profile, possibly associated with meltwater pulse 1B, which was sufficient to overstep the barrier and preserve the large volume of back-barrier material of unit 3. This is consistent with the steeper portion of the ravinement profile associated with this point of the shelf. The main shoreline complexes are punctuated to landward by a prominent and significantly flatter wave ravinement surface. This is indicative of two separate rates of ravinement.

The outer ravinement surface is more closely associated with rapid sea-level rise (i.e., meltwater pulse 1B), whereas the flatter inner ravinement surface is produced by slower rates of sea-level rise (cf. Davis and Clifton, 1987; Cattaneo and Steel, 2003). The hinge point corresponds to the proximal back-barrier of the overstepped 60 m shoreline, further lending credence to the idea that the steeper-sloped surface was a product of a faster rise in sea level.

Dates immediately above or below the ravinement surface, along the ravinement profile landward of this shoreline, show that from distal to proximal, the ravinement surface spanned an age range of ~6160 yr (Table 1). This implies a lengthy slowstand period that may have produced the several smaller shorelines to landward of the main shoreline complex (e.g., Fig. 3) and that accounts for their poor preservation as the shoreline transgressed the shore profile. The rate of sea-level rise is ~2.9 mm yr–1 along the ravinement profile, slightly faster than the slowstand rates observed by Kelley et al. (2010) for the Maine coast over the period 11.5–7.5 ka, yet still considered slow compared to the figures given by Storms et al. (2008) (10 mm yr–1) when modeling barrier response to rapid sea-level rise. Up the transgressive

profile, there is very little volumetric change in the back-barrier deposits. This is a result of the lessening antecedent gradient, which compensates for the increased erosion potential of subsequent slower ravinement (e.g., Lorenzo-Trueba and Ashton, 2014).

The preservation of small barrier remnants to landward of the hinge point (see Shoreline Genesis section) is especially associated with an inherently flatter ravinement surface (and thus increased erosive potential due to slow ravinement). Unlike the main barrier example, the lower antecedent gradients here are the controlling factor in enhancing the potential for overstepping. In this case, preservation of only incomplete barrier remnants can occur and manifest as smaller, less-prominent seafloor features (e.g., Figs. 3, 5, and 6, inset 1).

The sediment budget may also play a role in the retreat/overstepping of a barrier system (e.g., Storms and Swift, 2003). In light of the sediment-starved nature of this shelf, the overstepping of the barrier could be enhanced by the relative excess of newly created accommodation space linked to relative sea-level rise, as opposed to a situation where sediment supply is sufficient to replenish sediment lost from the barrier as it is transgressed (e.g., Mellett et al., 2012). In a deficit scenario, the paleoshoreface of the barrier is reworked, and the preserved portions of the barrier are merely remnants of a larger system. Green et al. (2013a) showed that for the most seaward, –60 m barrier, up to half of the barrier was reworked. The smaller barriers seaward of the –60 m barrier similarly represent a discontinuous retreat, with sporadic overstepping and preservation during low-sediment-supply conditions.

Influence of Antecedent Geology on Transgressive Stratigraphy

The contemporary shoreface is punctuated by several pinnacles of the postglacial barrier system. These have created impediments to the postravinement smoothing of the shoreface and have resulted in isolated packages of seawardonlapping shoreface material that were separated from the main shoreface package landward of 40 m as the shoreface was disconnected during sea-level rise. The steep shelf gradient would normally be expected to be associated with a thick postravinement sediment blanket (cf. Cattaneo and Steel, 2003); however, the thickest material accumulates over the flatter ravinement surface. We consider that the antecedent geology in the form of the barrier shorelines has exerted an overarching control on the Shoreface architecture and morphology by damming the seaward transfer of material during the ravinement process, together with further sheltering of the material from seaward-directed storm waves. Where the ravinement surface is steeper, this was punctuated by significant topographic obstacles that precluded a thick drape or healing wedge from developing, creating the sporadic and isolated deposits of subunit 4.1 instead.

Landward of the main barrier hinge line, thicker accumulation of material has occurred despite the lower-gradient setting, precisely due to the damming of material. This is further supplemented by relatively recent transfer of sediment over the barriers during storms and wave shoaling (subunit 4.3; e.g., Flemming, 1981).

The isolation of the lower shoreface deposits also implies a disconnection between the shore face and the landward-migrating surf zone, something at odds with the general models of coastal response to sea-level rise. These models assume that the surf zone–beachface and Shoreface migrate in tandem and at the same rates, and that the shoreface maintains a contiguous whole (e.g., Cowell et al., 1999). Our data show that it is possible to segregate

deposits of the lower shoreface from the upper shoreface where the barrier has survived the ravinement process and maintains a significant topographic expression on the lower shoreface. This may be a factor of the barrier's early lithification; however, a similar response is envisioned in particularly coarse-grained barrier settings where the barrier relaxation time is longer. This segregated material is likely to remain in the lower shoreface, where it is reworked by storm processes (e.g., subunit 4.2).

The presence of an older underlying shoreline may also have created a focal point for the development of more recent shorelines. Cooper et al. (2013) described a series of stacked shorelines, associated with several highstands from the Cretaceous to present day. A similar situation occurs in the submerged shorelines of Durban. The anchoring of a younger transgressive shoreline on an older regressive shoreline implies some form of dynamic influence on the position of the shoreline. We suggest that topographic highs of the older shoreline provided some localized sediment sources for the new shoreline, effectively removing the upstanding remnants of this older system. Conversely, the lower-lying points such as the lagoonal areas provided the requisite accommodation space for formation of the new shoreline.

General Implications for Sandy Barrier

Overstepping and Future Sea-Level Rise

We attribute the overstepping of the main barrier shoreline system to an initial rapid rise in relative sea level, which ameliorated the effects of an energetic wave base as it translated over a sandy barrier. To our knowledge, the only other example of an overstepped sandy

barrier is that of a system in the Adriatic documented by Storms et al. (2008). That system appears to have behaved similarly to the example presented in this paper, where rapid sea-level rise (associated with meltwater pulse 1A) initially overstepped the main barrier. Furthermore, overstepping was aided by increasing backbarrier accommodation, which was facilitated by a decrease in back-barrier gradient during a subsequent interval of slowly rising sea level (Storms et al., 2008). These two factors thus appear to be of key importance in the process of overstepping of sandy barrier systems.

This process is also aided by the early cementation of the barrier. Most of the intricately preserved submerged barrier shorelines that are identified from shelves worldwide appear to be hosted in areas where precipitation of calcium carbonate is rapid and early diagenesis can help to preserve the shoreline form. Examples include northern KwaZulu-Natal in South Africa (Salzmann et al., 2013), the inner shelf of western Sardinia (De Falco et al., 2015), the Florida shelf (Locker et al., 1996; Jarrett et al., 2005), and the northeast Gulf of Mexico (Gardner et al., 2007). In areas where the late Pleistocene– Holocene climate is unfavorable for early cementation, it is likely that these systems are not preserved as fully or in as much detail due to almost whole reworking during wave ravinement. In areas of similar Global Isostatic Adjustment (GIA) and climate, we expect shorelines to be found at similar depths and with a similar degree of preservation (e.g., Green et al., 2014).

In the steepest portions of the shelf sector (0.89°) that are associated with the fastest ravinement processes, the shoreline translated a distance of ~1600 m (Fig. 1). Assuming this was associated with the period of meltwater pulse 1B, where sea levels rose at a rate of 6 cm yr–1 (Liu and Milliman, 2004), this equates to an initial shoreline translation rate of 5 m yr–1. It appears that, coupled with these factors, this is the rate of shoreline migration that is

optimal to strand a partially cemented sandy barrier system and to disconnect the shoreface-beachface continuum.

The subsequent slower rate of shoreline migration (~2700 m over 6160 yr; 0.43 m yr–1) was still sufficient to overstep some sandy barriers, though they are only partially preserved. This is primarily due to the flatter profile (0.18°). In the context of future sea-level rises and climate change, the Intergovernmental Panel on Climate Change (IPCC) proposes a 0.3–0.6 m rise in sea level over the next 95 yr, assuming the lowest emission scenario (IPCC, 2014). Given the overall steep (0.6°) coastal profile of Durban, this equates to a rate of shoreline translation of between 0.28 and 0.57 m yr–1. It would thus appear that barrier overstepping on similar-gradient coastlines would be limited, and translation or erosion of the barrier would be a greater likelihood in the context of future rises in sea level.

CONCLUSIONS

In general, the shelf gradient plays an important role in the preservation of barrier shoreline deposits, and steeper gradients hinder the process of overstepping. Despite the steep shelf gradient and consistently high wave energy of the study area, barrier shoreline and back-barrier deposits have been remarkably well preserved through this process. The extent of preservation and the nature of the preserved deposits during sea-level rise over the coastal profile are dominantly controlled by the rate of sea-level rise. Early diagenesis is a secondary factor in the preservation of these shorelines. The main shoreline complex in the study is punctuated to landward by a prominent and significantly flatter wave ravinement surface. This is indicative of differential rates of ravinement, where the outer ravinement surface was associated with rapid sea-level rise (possibly meltwater pulse 1B), and the flatter inner

ravinement surface was produced by slower rates of relative sealevel rise. This rapid sea-level rise, coupled with localized depressions in the antecedent backbarrier topography, facilitated overstepping of the main barrier shoreline and back-barrier in this study. The smaller shorelines landward of the main –60 m shoreline are less well preserved and were overstepped by virtue of greater
accommodation and lower-gradient settings that outcompeted the slower rates of ravinement experienced in this portion of the shelf. The antecedent geology in the form of the barrier shorelines has exerted an overarching control on the shoreface architecture and morphology by damming the seaward transfer of material during the ravinement process and sheltering it from redistribution by contemporary storm waves. In light of climate change and future sealevel rise, the predicted rates of shoreline migration may be insufficient to cause contemporary shorelines with gradients comparable to Durban to be overstepped.

ACKNOWLEDGMENTS

We acknowledge the captain and crew of the RV Meteor, cruise M102, without whose capable efforts, data collection would have been impossible in extremely testing sea conditions. We further acknowledge our colleagues on the cruise, especially Shannon Dixon, Simon Mill, Jens Weiser, Martin Kugel, and Annette Hahn. We also acknowledge the Ethekweni Municipality/Environmental Mapping and Surveying for the bathymetry data shown in Figure 1. This project was funded under the auspices of Regional
Archives for Integrated iNvestigations (RAiN) and by a competitive research grant from the University of KwaZulu-Natal (UKZN). This work is a contribution to NERC project NE/H024301/1.

REFERENCES CITED

Belknap, D.F., and Kraft, J.C., 1981, Preservation potential of transgressive coastal lithosomes on the US Atlantic shelf: Marine Geology, v. 42, p. 429–442, doi: 10 .1016 /0025 -3227 (81)90173 -0 .

Birch, G.F., 1996, Quaternary sedimentation off the east coast of southern Africa (Cape Padrone to Cape Vidal): Bulletin of the Geological Survey of South Africa: Council for Geoscience, v. 118, p. 55.

Brenner, O.T., Moore, L.J., and Murray, A.B., 2015, The complex influences of back-barrier deposition, substrate slope and underlying stratigraphy in barrier island response to sea level rise: Insights from the Virginia Barrier Islands, Mid-Atlantic Bight, U.S.A.: Geomorphology, v. 246, p. 334–350, doi: 10 .1016 /j.geomorph .2015 .06 .014 .

Brooke, B.P., Olley, J.M., Pietsch, T., Playford, P.E., Haines, P.W., Murray-Wallace, C.V., and Woodroffe, C.D., 2014, Chronology of Quaternary coastal aeolianite deposition and the drowned shorelines of southwestern Western Australia—A reappraisal: Quaternary Science Reviews, v. 93, p. 106–124, doi: 10 .1016 /j .quascirev .2014 .04 .007 .

Carter, R.M., Carter, L., and Johnson, D.P., 1986, Submergent shorelines in the SW Pacific: Evidence for an episodic post-glacial transgression: Sedimentology, v. 33, p. 629–649, doi: 10 .1111 /j .1365 -3091 .1986 .tb01967 .x .

Cattaneo, A., and Steel, R.J., 2003, Transgressive deposits: A review of their variability: Earth-Science Reviews, v. 62, p. 187–228, doi: 10 .1016 /S0012 -8252 (02)00134 -4 .

Cawthra, H.C., Neumann, F.H., Uken, R., Smith, A.M., Guastella, L.A., and Yates, A., 2012, Sedimentation on the narrow (8 km wide), oceanic current–influenced continental shelf off Durban, Kwazulu-Natal, South Africa: Marine Geology, v. 323–325, p. 107–122, doi: 10 .1016 /j .margeo .2012 .08 .001 .

Cooper, J.A.G., 1993, Sedimentation in a river-dominated estuary: Sedimentology, v. 40, p. 979–1017, doi: 10.1111 /j .1365 -3091 .1993 .tb01372 .x .

Cooper, J.A.G., and Pilkey, O.H., 2004, Sea-level rise and shoreline retreat: Time to abandon the Bruun rule: Global and Planetary Change, v. 43, p. 157–171, doi: 10 .1016 /j .gloplacha .2004 .07 .001 .

Cooper, J.A.G., Green, A.N., and Wright, I.C., 2011, Evolution
of an incised valley coastal plain estuary under low sediment supply: A ‘give-up’ estuary: Sedimentology, v. 59, p. 899–916, doi: 10 .1111 /j .1365 -3091 .2011 .01284 .x .

Cooper, J.A.G., Green, A.N., and Smith, A.M., 2013, Vertical stacking of multiple highstand shoreline deposits from the Cretaceous to the present: Facies development and preservation: Journal of Coastal Research, Special Issue, v. 65, p. 1904–1908.

Cowell, P.J., Hanslow, D.J., and Meleo, J.F., 1999, The shoreface, in Short, A.D., ed., Handbook of Beach andShoreface Morphodynamics: Chichester, UK, Wiley, p. 37–71.

Dabrio, C.J., Zazo, C., Goy, J.L., Sierro, F.L., Borja, F., Lario, J., Gonzalez, J.A., and Flores, J.A., 2000, Depositional history of estuarine infill during the last postglacial transgression (Gulf of Cadiz, southern Spain): Marine Geology, v. 162, p. 381–404, doi: 10 .1016/S0025 -3227 (99)00069 -9.

Davis, R.A., and Clifton, H.E., 1987, Sea-level change and the preservation potential of wave dominated and tide-dominated coastal sequences, in Nummedal, D., Pilkey, O.H., and Howard, J.D., eds., Sea-Level Fluctuation and Coastal Evolution: Society of Economic Paleontologists and Mineralogists Special Publication 41, p. 167–178, doi: 10 .2110 /pec .87 .41 .0167 .

De Falco, G., Antonioli, F., Fontolan, G., Lo Presti, V., Simeone, S., and Tonielli, R., 2015, Early cementation and accommodation space dictate the evolution of an overstepping barrier system during the Holocene: Marine Geology, v. 369, p. 52–66.

Engelhart, S.E., Horton, B.P., Douglas, B.C., Peltier, W.R., and Törnqvist, T.E., 2009, Spatial variability of late Holocene and 20th century sea-level rise along the Atlantic coast of the United States: Geology, v. 37, p. 1115–1118.

Felhaber, T.A., 1984, The Geochemistry and Sedimentology of Quaternary Shelf Sediments of the Tugela River, Natal, South Africa [Ph.D. thesis]: Cape Town, South Africa, University of Cape Town, 237 p.

Flemming, B.W., 1981, Factors controlling shelf sediment dispersal along the south-east African continental margin: Marine Geology, v. 42, p. 259–277, doi: 10 .1016/0025 -3227 (81)90166 -3 .

Flemming, B.W., and Hay, E.R., 1988, Sediment distribution and dynamics on the Natal continental shelf, in Schumann, E.H., ed., Coastal Ocean Studies off Natal, South Africa: Lecture Notes on Coastal and Estuarine Studies: Berlin, Springer-Verlag, p. 47–80, doi: 10.1007 /978 -1 -4757 -3908 -4_3 .

Forbes, D.L., Orford, J.D., Carter, R.W.G., Shaw, J., and Jennings, S.C., 1995, Morphodynamic evolution, selforganisation, and instability of coarse-clastic barriers on paraglacial coasts: Marine Geology, v. 126, p. 63–85, doi: 10 .1016 /0025 -3227 (95)00066 -8 .

Gardner, J.V., Calder, B.R., Hughes Clark, J.E., Mayer, L.A., Elston, G., and Rzhanov, Y., 2007, Drowned shelf-edge deltas, barrier islands and related features along the outer continental shelf north of the head of De Soto Canyon, NE Gulf of Mexico: Geomorphology, v. 89, p. 370–390, doi: 10 .1016 /j .geomorph .2007 .01 .005 .

Goff, J.A., Allison, M.A., and Gulick, S.P.S., 2010, Offshore transport of sediment during cyclonic storms: Hurricane Ike (2008), Texas Gulf Coast, USA: Geology, v. 38, p. 351–354, doi: 10 .1130 /G30632 .1 .

Green, A.N., and Garlick, L., 2011, A sequence stratigraphic framework for a narrow, current-swept continental shelf: The Durban Bight, central KwaZulu-Natal, South Africa:

Journal of African Earth Sciences, v. 60, p. 303–314, doi: 10 .1016 /j .jafrearsci .2011 .03 .007 .

Green, A.N., and MacKay, F., 2016, Unconsolidated sediment distribution patterns of the KwaZulu-Natal Bight: The role of wave ravinement in separating relict versus passive sediment populations: African Journal of Marine Science (in press).

Green, A.N., and Uken, R., 2005, First observations of sealevel indicators related to glacial maxima at Sodwana Bay, northern KwaZulu-Natal: Research in action: South African Journal of Science, v. 101, p. 236–238.

Green, A.N., Ovechkina, M.N., and Mostovski, M.B., 2012, Late Holocene shoreface evolution of the wave-dominated Durban Bight, KwaZulu-Natal, South Africa: A mixed storm and current driven system: Continental Shelf Research, v. 49, p. 56–64, doi: 10 .1016 /j .csr .2012.09 .003 .

Green, A.N., Cooper, J.A.G., Leuci, R., and Thackeray, Z., 2013a, Formation and preservation of an overstepped segmented lagoon complex on a high-energy continental shelf: Sedimentology, v. 60, p. 1755–1768, doi: 10.1111 /sed .12054 .

Green, A.N., Dladla, N.N., and Garlick, L., 2013b, The evolution of incised valley systems from the Durban continental shelf, KwaZulu-Natal, South Africa: Marine Geology, v. 335, p. 148–161, doi: 10 .1016 /j .margeo.2012 .11 .002 .

Green, A.N., Cooper, J.A.G., and Salzmann, L., 2014, Geomorphic and stratigraphic signals of postglacial meltwater pulses on continental shelves: Geology, v. 42, p. 151–154, doi: 10 .1130 /G35052 .1 .

Intergovernmental Panel on Climate Change (IPCC), 2014, Climate Change 2014: Synthesis Report. Contribution of Working Groups I, II and III to the Fifth Assessment Report of the Intergovernmental Panel on Climate Change [Core Writing Team, R.K. Pachauri and L.A. Meyer, eds.]: Geneva, Switzerland, IPCC, 151 p.

Jarrett, B.D., Hine, A.C., Halley, R.B., Naar, D.F., Locker, S.D., Neumann, A.C., Twichell, D., Hu, C., Donahue, B.T., Jaap, W.C., Palandro, D., and Ciembronowicz, K., 2005, Strange bedfellows—A deep-water hermatypic coral reef superimposed on a drowned barrier island; southern Pulley Ridge, SW Florida platform margin: Marine Geology, v. 214, p. 295–307, doi: 10.1016 /j .margeo .2004 .11 .012 .

Kelley, J.T., Belknap, D.F., Kelley, A.R., and Claesson, S.H., 2010, Drowned coastal deposits with associated archaeological remains from a sea-level slowstand: Northwestern Gulf of Maine, USA: Geology, v. 38, p. 695–698, doi: 10 .1130 /G31002 .1 . Kennett, J.P., 1982, Marine Geology: Englewood Cliffs, New Jersey, Prentice-Hall, Inc., 813 p.

Liu, J.P., and Milliman, J.D., 2004, Reconsidering meltwater pulses 1-A and 1-B: Global impacts of rapid sea-level rise: Journal of Ocean University of China [Oceanic and Coastal Sea Research], v. 3, p. 183–190, doi: 10 .1007 /s11802 -004 -0033 -8 .

Locker, S.D., Hine, A.C., Tedesco, L.P., and Shinn, E.A., 1996, Magnitude and timing of episodic sea-level rise during the last deglaciation: Geology, v. 24, p. 827–830, doi: 10 .1130 /0091 -7613 (1996)024 <0827:MATOES>2 .3 .CO;2 .

Lorenzo-Trueba, J., and Ashton, A.D., 2014, Rollover, drowning, and discontinuous retreat: Distinct modes of barrier response to sea-level rise arising from a simple morphodynamic model: Journal of Geophysical Research– Earth Surface, v. 119, p. 779–801, doi: 10 .1002/2013JF002941 .

Martin, A.K., and Flemming, B.W., 1987, Aeolianites of the South African coastal zone and continental shelf as sea-level indicators: South African Journal of Science, v. 83, p. 597–598.

Martin, A.K., and Flemming, B.W., 1988, Physiography, structure and geological evolution of the Natal continental shelf, in Schumann, E.H., ed., Coastal Ocean Studies off Natal, South Africa: Lecture Notes on Coastal and Estuarine Studies: Berlin, Springer-Verlag, p. 11–46, doi: 10 .1007 /978 -1 -4757 -3908 -4_2 .

Mellett, C.L., Hodgson, D.M., Lang, A., Mauz, B., Selby, I., and Plater, A.J., 2012, Preservation of a drowned gravel barrier complex: A landscape evolution study from the north-eastern English Channel: Marine Geology, v. 315–318, p. 115–131, doi: 10 .1016 /j .margeo.2012 .04 .008 .

Milne, G.A., and Mitrovica, J.X., 2008, Searching for eustasy in deglacial sea-level histories: Quaternary Science Reviews, v. 27, p. 2292–2302, doi: 10 .1016 /j.quascirev .2008 .08 .018 .

Moes, H., and Rossouw, M., 2008, Considerations for the utilization of wave power around South Africa: Workshop on Ocean Energy, Centre for Renewable and Sustainable Energy Studies Abstracts, Stellenbosch, South Africa, 21 February.

Nichol, S., Zaitlin, B., and Thom, B., 1997, The upper Hawkesbury River, New South Wales, Australia: A Holocene example of an estuarine bayhead delta: Sedimentology, v. 44, p. 263–286, doi: 10 .1111 /j .1365 -3091.1997 .tb01524 .x .

Ramsay, P.J., 1994, Marine geology of the Sodwana Bay shelf, southeast Africa: Marine Geology, v. 120, p. 225–247, doi: 10 .1016 /0025 -3227 (94)90060 -4 .

Ramsay, P.J., and Cooper, J.A.G., 2002, Late Quaternary sea-level change in South Africa: Quaternary Research, v. 57, p. 82–90, doi: 10 .1006 /qres .2001 .2290 .

Ramsey, B.C., 2001, Development of the radiocarbon calibration program OxCal: Radiocarbon, v. 43, p. 355–363.

Reimer, P.J., Bard, E., Bayliss, A., Beck, J.W., Blackwell, P.G., Bronk-Ramsey, C., Buck, C.E., Cheng, H., Edwards, R.L., and Friedrich, M., 2013, IntCal13 and Marine13 radiocarbon age calibration curves 0–50,000 years cal BP: Radiocarbon, v. 55, p. 1869–1887, doi: 10 .2458 /azu_js_rc .55 .16947 .

Richardson, A.G., 2005, The Marine Geology of the Durban Bight [M.Sc. thesis]: Durban, South Africa, University of KwaZulu-Natal, 169 p.

Salzmann, L., Green, A.N., and Cooper, J.A.G., 2013, Submerged barrier shoreline sequences on a high energy, steep and narrow shelf: Marine Geology, v. 346, p. 366–374, doi: 10 .1016 /j .margeo .2013 .10 .003 .

Shepard, F.P., 1963, Submarine Geology: New York, Harper and Row, 557 p.

Storms, J.E.A., and Swift, D.J.P., 2003, Shallow-marine sequences as the building blocks of stratigraphy: Insights from numerical modelling: Basin Research, v. 15, p. 287–303, doi: 10 .1046 /j .1365 -2117 .2003 .00207 .x .

Storms, J.E.A., Weltje, G.J., Terra, G.J., Cattaneo, A., and Trincardi, F., 2008, Coastal dynamics under conditions of rapid sea-level rise: Late Pleistocene to early Holocene evolution of barrier-lagoon systems on the northern Adriatic shelf (Italy): Quaternary Science Reviews, p. 27, p. 1107–1123.

Thieler, E.R., and Ashton, A.D., 2011, ‘Cape capture’: Geologic data and modeling results suggest the Holocene loss of a Carolina Cape: Geology, v. 39, p. 339–342, doi: 10 .1130 /G31641 .1 .

Zecchin, M., and Catuneanu, O., 2013, High-resolution sequence stratigraphy of clastic shelves I: Units and bounding surfaces: Marine and Petroleum Geology, v. 39, p. 1–25, doi: 10 .1016 /j .marpetgeo .2012 .08 .015 .

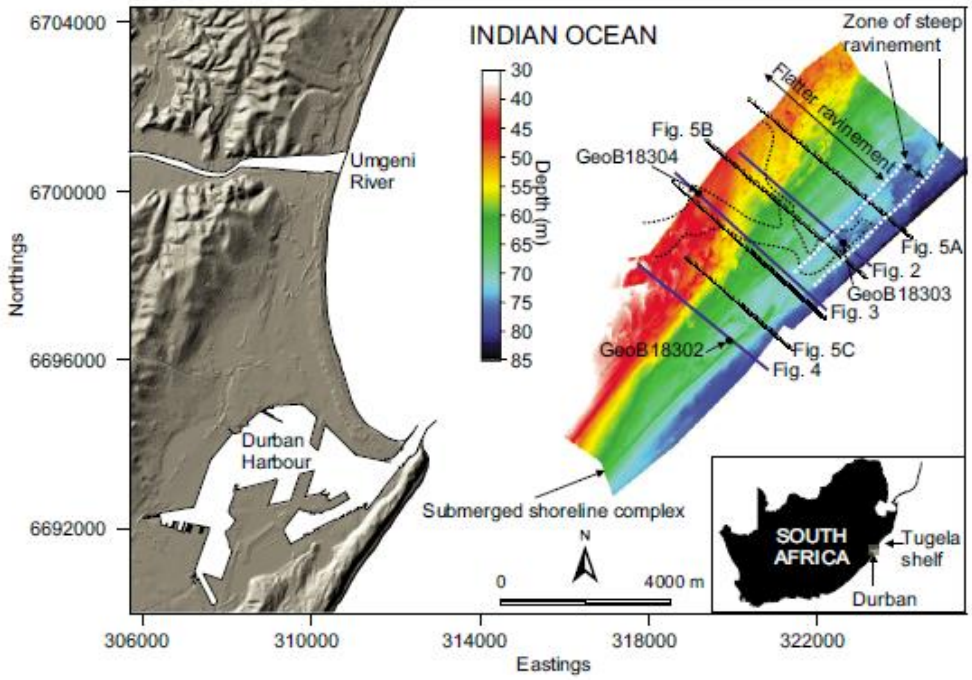

Figure 1. Locality map detailing sun-shaded and color-coded bathymetry of the submerged shoreline complex (after Green et al., 2013a). Note the main barrier developed at ~60 m water depth. Superimposed are the various seismic-reflection profiles (heavy lines denote Parasound data) and core localities. Dashed lines show incised valley position identified by Green et al. (2013a). White dashed lines show the zone of steepest ravinement, landward of which is a flatter ravinement profile. Coordinate system in eastings and northings, UTM 36S.

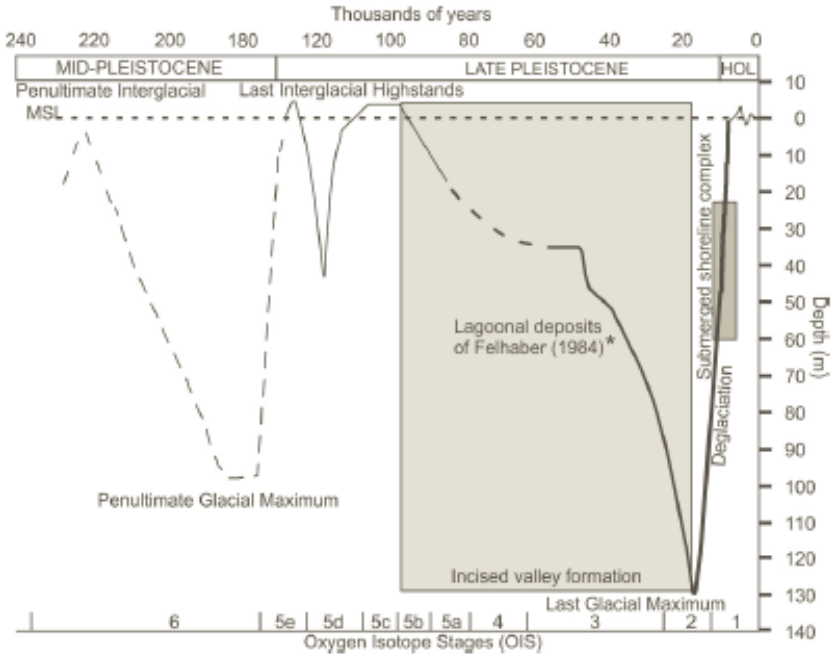

Figure 2. Relative sea-level fluctuations from the east coast of South Africa (after Ramsay and Cooper, 2002). Note the date and depth of the lagoonal deposit identified by Felhaber (1984) from the neighboring Tugela shelf and the depth range of the submerged shoreline complex described in this paper. MSL—mean sea level; HOL—Holocene.

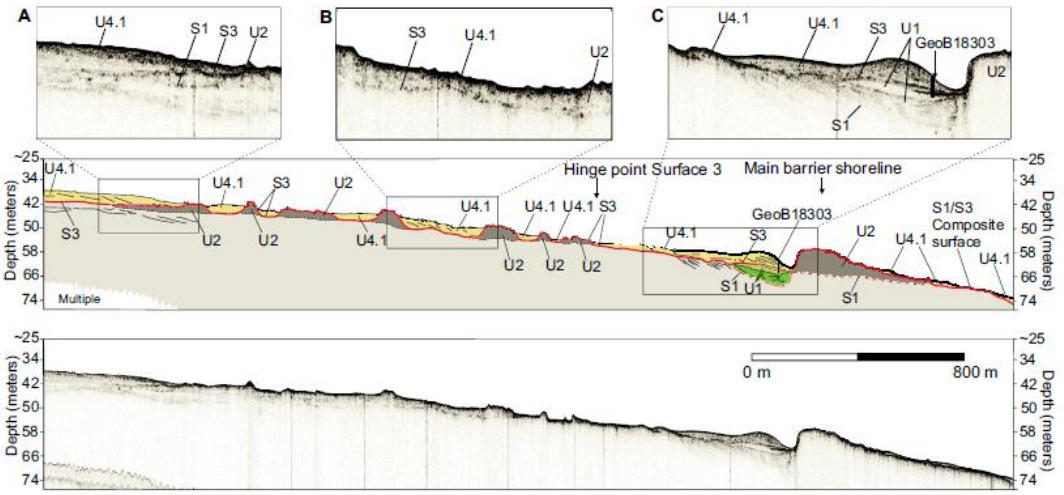

Figure 3. Shore-perpendicular seismic section and interpretation showing an uneven, high-amplitude reflector (surface 3) occurring across the midshelf that truncates the underlying Cretaceous-age strata. Expanded areas show: (A) Subunit 4.1, comprising a package of continuous, moderate-amplitude, seaward-prograding, sigmoid reflectors that downlap surface 3. (B) Subunit 4.1, resting on surface 3, between two saddles of unit 2. (C) An incised valley, outlined by surface 1, where the valley hosts a valley fill sequence (unit 1) and is truncated by surface 3. Subunit 4.1 onlaps surface 3. Note the intersection of core GeoB18303 with subunit 4.1 and a small portion of unit 1.

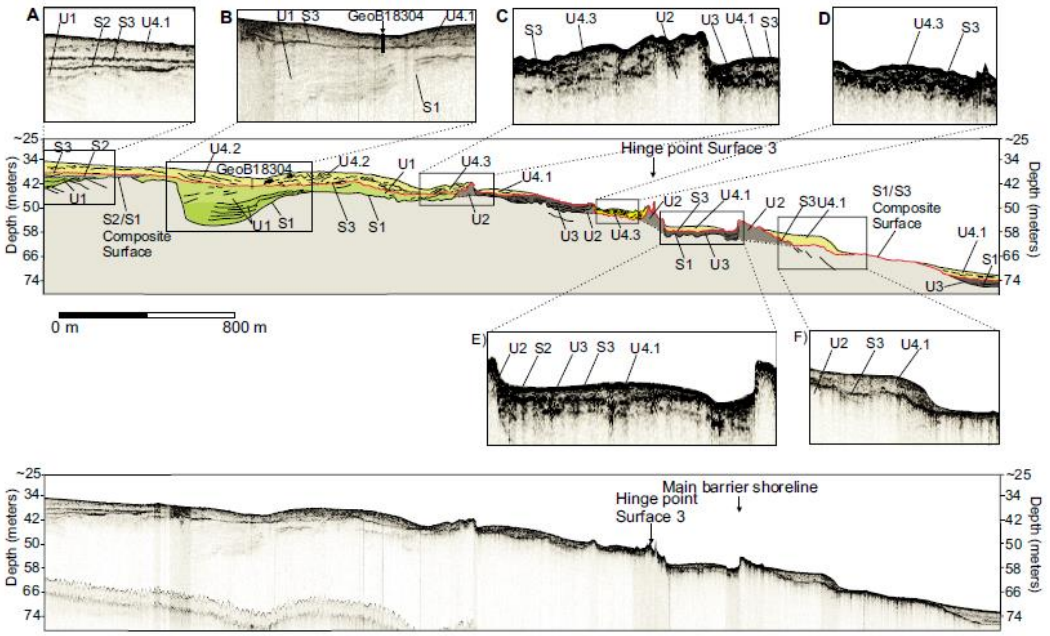

Figure 4. Shore-perpendicular seismic section and interpretation. Expanded areas show: (A) An incised valley within surface 1, the proximal location of surface 2, and the truncating nature of surface 3. (B) The position of core GeoB18304 where it penetrates units 1 and 4.2. (C) The onlapping nature of subunit 4.3 with unit 2. Note that this point of the shelf profile marks the hinge point in the gradient of surface 3. (D) Draping of subunit 4.3 between two saddles of unit 2. (E) Unit 3 resting on a relatively horizontal surface 1. (F) Aggrading/prograding subunit 4.1 onlapping unit 2 and prograding over the Cretaceous basement.

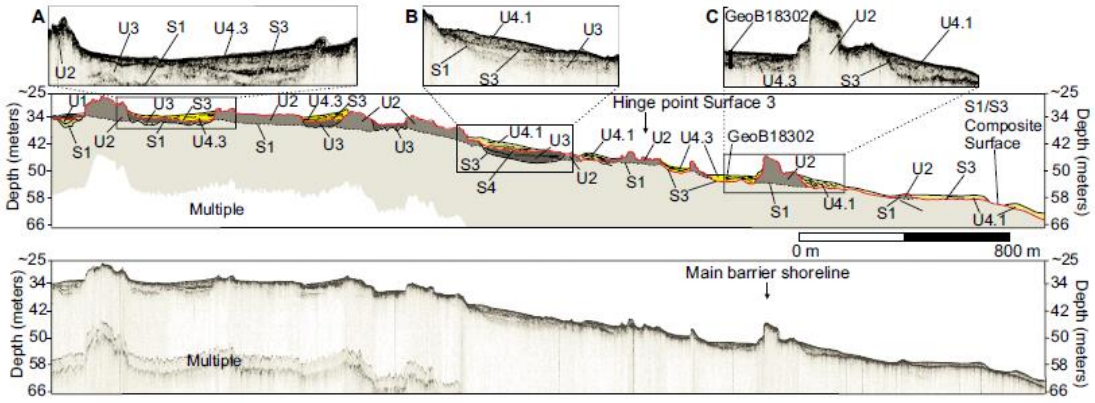

Figure 5. Shore-perpendicular seismic sections and interpretation. Note the dominant occurrence of unit 2 at 60 m depth. Expanded areas show: (A) Unit 3 resting on surface 1. Subunit 4.3 rests on surface 3, between two saddles of unit 2. (B) The erosional truncation of unit 3 by surface 3. Subunit 4.1 is seaward prograding and onlaps surface 3. (C) Note the seaward-prograding nature of subunit 4.1 and the position of core GeoB18302.

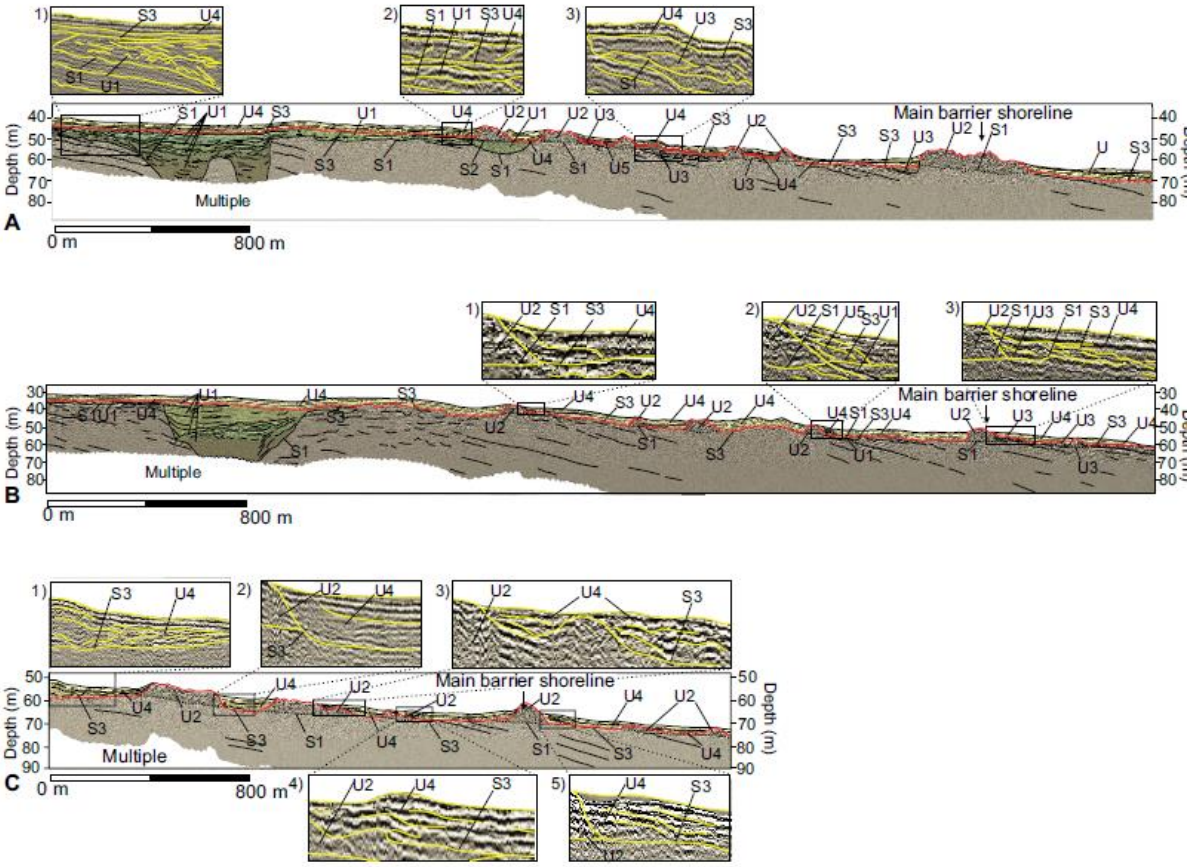

Figure 6. Shore-perpendicular boomer seismic sections and interpretive overlay from the Durban central basin. (A) Inset 1: Prominent incised valley filled by unit 1. Flat-lying unit 4 overlies surface 3. Inset 2: Unit 4 onlapping unit 2 with landward-prograding reflectors. Inset 3: Unit 3 saddling between two ridges of unit 2, truncated by surface 3 and overlain by unit 4. (B) Inset 1: Unit 4 onlaps surface 3 with seaward-dipping internal reflectors. Inset 2: Unit 4 onlaps surface 3 with seaward-dipping internal reflectors. Inset 3: Preserved back-barrier deposits overlain by Unit 4. (C) Inset 1: Unit 4 rests on surface 3, with a chaotic basal seismic reflector configuration, becoming more parallel in upper portions of the unit. Inset 2: Unit 4 saddling two ridges of unit 2, onlapping surface 3 at the landward ridge. Inset 3: Unit 2 draped by unit 4 sediment. Unit 4 shows a seaward-prograding internal reflector configuration. Insets 4 and 5 show similar geometries as inset 3.

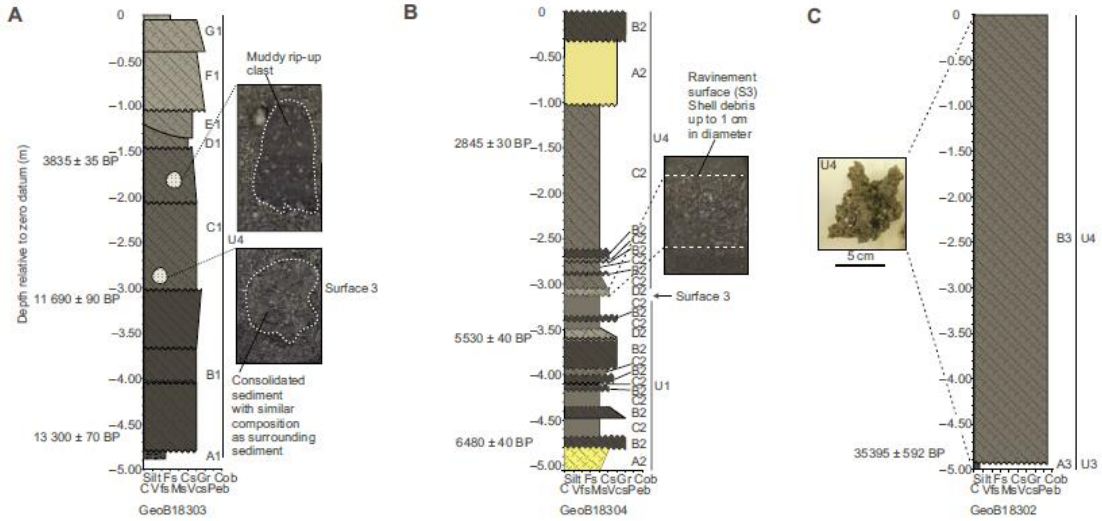

Figure 7. Core logs taken at locations indicated in Figures 1–4. C14 dates are indicated at their respective depths. (A) Core GeoB18303, which penetrated unit 4 only. Note the muddy rip-up clast and a clump of consolidated sediment similar in composition to the surrounding material. (B) Core GeoB18304, which penetrated units 1 and 4. Note the distinct layer of shell debris with fragments reaching 1 cm in diameter, corresponding to surface 3. (C) Core GeoB18302, which penetrated the upper levels of a stiff muddy deposit and a 4.9-m-thick portion of unit 4 (calcareous rubble facies). C—clay, VFS—very fine sand, FS—fine sand, MS—medium sand, CS—coarse sand, VCS—very coarse sand, Gr—granule, Peb—pebble, Cob—cobble.

TABLE 1. CORE SAMPLE INTERVALS, KEY ACCELERATOR MASS SPECTROMETRY (AMS) RADIOCARBON DATES, DATED MATERIAL, SAMPLE CONTEXT, AND CORRELATIONS BETWEEN CORE SEDIMENTOLOGY AND STRATIGRAPHIC UNITS OR SURFACES

Core and interval (cm)	Calibrated AMS radiocarbon age (cal yr B.P.)	Sample material	Depth range	Corresponding unit/surface	Interpretation
GeoB18303, 182.5	3835 ± 35	Bulk organic carbon	–	Subunit 4.1	Rip-up clast
GeoB18303, 340	11,690 ± 90	Bulk organic carbon	–	Unit 1/surface 3	Incised valley fill, flood tide deltaic package, underlying surface 3 (wave ravinement surface)
GeoB18303, 489	13,300 ± 70	Bulk organic carbon	–	Unit 1	Incised valley fill, central estuarine basin
GeoB18304, 145	2845 ± 30	Single gastropod, *Nassarius* sp.	Sublittoral	Subunit 4.1	Prograding shoreface
GeoB18304, 359	5530 ± 40	Articulated bivalve, life position, *Eumarcia paupercula*	Open sandy intertidal	Surface 3	Just beneath capping horizon between incised valley fill (unit 1) and prograding shoreface (subunit 4.1), wave ravinement surface
GeoB18304, 476	6480 ± 40	Articulated bivalve, life position, *Eumarcia paupercula*	Open sandy intertidal	Subunit 1	Upper incised valley fill, likely to represent flood tide deltaic sand body
GeoB18302, 515	35,395 ± 592	Bulk organic carbon	–	Not resolved	Lagoonal clay

TABLE 2. SEISMIC STRATIGRAPHY DETAILING UNIT MORPHOLOGY, INTERNAL REFLECTOR CHARACTERISTICS, BOUNDING SURFACES, AND INTERPRETATION

Unit		Underlying surface	Description	Stratal relationship	Thickness (m)	Interpreted depositional environment
Unit 4	4.3	S2	Landward-prograding isolated wedges	Continuous, moderate-amplitude, landward-prograding, oblique parallel to divergent reflectors	3	Storm overwash
	4.2	S3	Land-attached sediment wedge	Discontinuous, moderately high-amplitude contorted to segmented subparallel reflectors	4	Reworked shoreface
	4.1	S2	Prograding sediment wedge	Continuous, moderate-amplitude, seaward-prograding, sigmoid reflectors. In some locations, low- to moderate-amplitude, sparsely spaced, subhorizontal, subparallel reflectors	4	Prograding shoreface
Unit 3		S2	Drape package bound on either side by high-relief pinnacle structures	Acoustically opaque reflectors in parasound, moderate-amplitude shingled reflector configuration in boomer	3.75	Back-barrier lagoonal deposit
Unit 2		S2	High-relief pinnacle structures welded onto basement rock	High-relief, unclear internal structure	8.5	Barrier system
Unit 1		S1	Well-developed onlapping drape package	Moderate-amplitude, chaotic to draped parallel reflectors	8.5	Incised valley